

Why does $B_{12}H_{12}$ -icosahedron need two electrons to be stable: A first-principles electron-correlated investigation of $B_{12}H_n$ ($n=6,12$) clusters

Pritam Bhattacharyya,^{*,†} Ihsan Boustani,^{*,‡} and Alok Shukla^{*,†}

[†]*Department of Physics, Indian Institute of Technology Bombay, Powai, Mumbai 400076, India*

[‡]*Theoretical and Computational Chemistry, Faculty of Mathematics and Natural Sciences, Bergische Universität, Wuppertal, Gauss Strasse 20, D-42097 Wuppertal, Germany*

E-mail: pritambhattacharyya01@gmail.com; boustani@uni-wuppertal.de; shukla@phy.iitb.ac.in

Abstract

In this work, we present large-scale electron-correlated computations on various conformers of $B_{12}H_{12}$ and $B_{12}H_6$ clusters, to understand the reasons behind the high stability of di-anion icosahedron (I_h) and cage-like $B_{12}H_6$ geometries. Although the B_{12} -icosahedron is the basic building block in some structures of bulk boron, it is unstable in its free form. Furthermore, its H-passivated entity, i.e., $B_{12}H_{12}$ icosahedron is also unstable in free form. However, dianion $B_{12}H_{12}$ has been predicted to be stable as a perfect icosahedron in the free-standing form. In order to capture the correct picture for the stability of $B_{12}H_{12}^{-2}$ and $B_{12}H_6$ clusters, we optimized these structures by employing the coupled-cluster singles-doubles (CCSD) approach and cc-pVDZ basis set. We also performed vibrational frequency analysis of the isomers of these clusters,

using the same level of theory to ensure the stability of the structures. For all the stable geometries obtained from the vibrational frequency analysis, we additionally computed their optical absorption spectra using the time-dependent density functional theory (TDDFT) approach, at the the B3LYP/6-31G* level of theory. Our calculated absorption spectra could be probed in future experiments on these clusters.

Introduction

Boron, with one electron less than carbon, has unique bonding properties, giving rise to several allotropes and compounds, with diverse physical and electronic characteristics.¹ In contrast to the solid carbon and carbon hydrides, which occur in nature abundantly in the form of graphite, diamond, or hydrocarbons, solid boron as well as boron hydrides (called boranes) do not exist in nature, and must be synthesized in the lab. Besides γ -B₂₈ boron, the well known boron solids α - and β -rhombohedral boron are composed of B₁₂ icosahedra. Even though the basic building block unit in solid boron is a B₁₂ icosahedron, it is unstable in isolated form due to the partly-filled, degenerate, highest-occupied molecular orbitals (HOMOs). This leads to a symmetry reduction by the Jahn-Teller-Effect, transforming the 3D icosahedral I_h-symmetry into a quasi-planar 2D C_{3v}-symmetry, with six delocalized π -electrons, analogous to benzene.² Nevertheless, the B₁₂ icosahedron plays a very important role in the boron chemistry, which began to emerge in the early 20th century, with the efforts aimed at exploring the possible synthesis of boranes, in analogy with the hydrocarbons. By the middle of the 20th century, some boron hydride compounds were synthesized exhibiting high thermal capacity, which on burning could release huge quantities of heat, proving to be excellent fuel sources, just like hydrocarbons. It is well known that the geometries of boranes, i.e., boron hydrides of the form of B_xH_y, are classified in closo, nido, and arachno structures. Furthermore, Lipscomb proposed in 1992, that large closo boron hydrides forming polyhedral boranes in analogy to carbon fullerenes, can be constructed.³ The most prominent and well known borane is the dodecahydro-closo-dodecaborate B₁₂H₁₂²⁻

di-anion, which also possesses an icosahedral structure, but with an extremely high stability. This fact leads to the question whether all structures of boranes depend on the content of the hydrogen atoms and whether their chemical properties are tunable through the number of the participating hydrogen atoms, and whether they can affect and control the chemical reactivity. Ohishi *et al.*⁴⁻⁶ investigated the formation of hydrogen-content-controlled $B_{12}H_n^+$ clusters experimentally through the decomposition and the ion-molecule reaction of the decaborane $B_{10}H_{2m}^+$ (with $m = 1 - 6$) and diborane B_2H_6 molecules. They found that the detachment of hydrogen atoms leads to an energy barrier for a structural transition. They also confirmed that $B_{12}H_n^+$ clusters with more hydrogen atoms ($n = 7 - 12$) prefer the icosahedral structures, while the clusters with fewer hydrogen atoms ($n = 0 - 6$) favor planar structures. Later on, Szwacki *et al.*⁷ proposed a benzene-like structure $B_{12}H_6$ called borozene, while Sahu and Shukla⁸ investigated the aromaticity of borozene, and computed its electronic properties and optical absorption spectrum, along with the static polarizability. Forte *et al.*⁹ predicted larger aromatic compounds composed of up to 26 borozene molecules in analogy to the case of polycyclic aromatic hydrocarbons such as coronene and coronene 19, for which the basic building block is benzene. To make the analogy complete, they also reported that the dangling bonds of these boron clusters are saturated by hydrogen atoms.⁹

Here, we present a large-scale first-principles quantum-chemical study of various isomers of $B_{12}H_{12}$ and B_2H_6 clusters, with the motivation to investigate the reasons behind the high stability of di-anion icosahedron (I_h) and cage-like $B_{12}H_6$ geometries. It is important to understand as to why the neutral $B_{12}H_{12}$ -icosahedron is unstable, while in some structures of bulk boron, B_{12} -icosahedron is the basic unit. In order to understand the relationship between the geometry and optical properties of these clusters, we also computed the optical absorption spectra of all the stable isomers using the TDDFT approach, at the B3LYP/6-31G* level of theory. We believe that ours is the first study of its kind probing the stability and the optical properties of boranes, within a first-principles formalism.

Theoretical approach and Computational details

We performed the geometry optimization of various isomers of $B_{12}H_n$ ($n = 6, 12$) clusters by employing the coupled-cluster singles-doubles (CCSD) approach and cc-pVDZ basis set. All the calculations were carried out using the GAUSSIAN 16 computer program.¹⁰ On examining the many-electron wave functions of the final optimized states, we found that the restricted closed-shell Hartree-Fock configuration dominates the ground state wave functions of all the considered $B_{12}H_{12}$ and $B_{12}H_6$ isomers. Therefore, a single-reference electron-correlation approach such as CCSD employing the HF state as reference, will yield reasonable results. Single point energy was also computed at the obtained optimized geometries, using the coupled-cluster singles-doubles with perturbative triples (CCSD(T)) method, and the cc-pVTZ basis set to improve the inclusion of electron-correlation effects. The optimized geometries of various neutral isomers of $B_{12}H_{12}$ and $B_{12}H_6$ are presented in Figs. 1 and 2, respectively. Additionally, Fig. 1 also exhibits the optimized structure of dianion $B_{12}H_{12}^{-2}$. The calculated ground state energy, correlation energy, and average binding energy per atom, all computed using the CCSD(T) approach, for each isomer are presented in the Table 1. The correlation energy is the difference of energy computed at the CCSD(T) and the Hartree-Fock energy for a given system. The binding energy which can ensure the stability of a system was calculated using the following formula

$$\frac{E_{BE}}{N} = \frac{N_B}{N} E_B + \frac{N_H}{N} E_H - \frac{E_T}{N}, \quad (1)$$

where N_B and N_H are the respective numbers of boron and hydrogen atoms present in the system, while E_B and E_H are the energies of single boron and hydrogen atoms, respectively. N is the total number of atoms present in the system, whereas E_T is the total energy of the system. Here, E_B and E_H were taken to be -24.598101 Hartree, and -0.4998098 Hartree, respectively, computed using the CCSD(T) method, and the cc-pVTZ basis set.

Furthermore, we performed the vibrational frequency analysis of the conformers of $B_{12}H_{12}$

and $B_{12}H_6$ clusters using the CCSD approach, along with the cc-pVDZ basis set to verify their stability. We find that all the isomers of $B_{12}H_{12}$ cluster are unstable, while those of the $B_{12}H_6$ cluster are stable. To further confirm our results on the instability of $B_{12}H_{12}$ isomers, we also optimized and calculated their vibrational frequencies using the density-functional theory (DFT), and all the isomers, except a "deformed chain" structure, were found to be unstable.

Next, we computed the optical absorption spectra of the stable structures of all the clusters using the time-dependent density functional theory (TDDFT) approach. For the purpose, we employed the hybrid exchange-correlation functional, B3LYP,¹¹⁻¹³ and a localized Gaussian basis set, 6-31+G*, which is composed of a valance double- ζ set, augmented with s and p diffuse functions, and d polarization functions for the non-hydrogen atoms. Although, the B3LYP hybrid functional was mainly developed for ground-state calculations, but it has also been found to yield accurate results on the excited states of both closed-shell,¹⁴ and open-shell systems.^{15,16} In some of the recent studies, it has been found that the above computational framework (B3LYP\6-31+G*) for both, ground and excited states led to high-accuracy results, in excellent agreement with the experiments for the π -conjugated aromatic hydrocarbon molecules.¹⁷⁻²⁰ We adopted the TDDFT approach to compute the optical properties of the stable structures, because of the two primary reasons: (i) earlier studies exhibit reliable performance, and (ii) computing the optical absorption using wave-function-based electron-correlated approaches is computationally quite prohibitive, for the relatively larger clusters considered in this work. Therefore, we performed the ground state calculations using the most accurate electron-correlated approach (coupled-cluster approach), while the excited-state calculations were carried out by employing the TDDFT methodology.

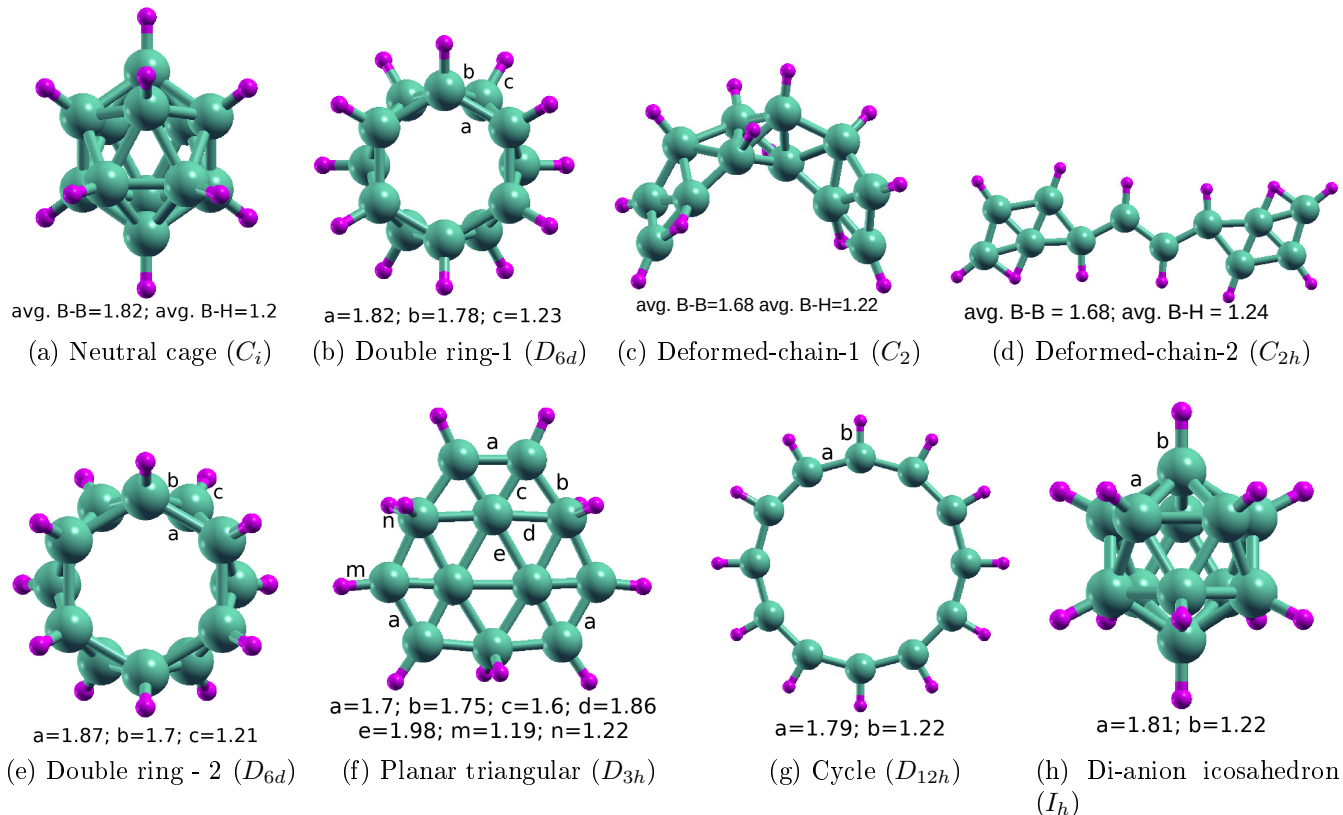


Figure 1: Optimized geometries of the various isomers of $B_{12}H_{12}$ cluster, obtained using the CCSD approach, and the cc-pVDZ basis set. The atoms with purple color indicate the hydrogen atoms, and the rest of them are boron atoms. The point group symmetry of each isomer is written in parentheses. All the bond lengths are in Å unit.

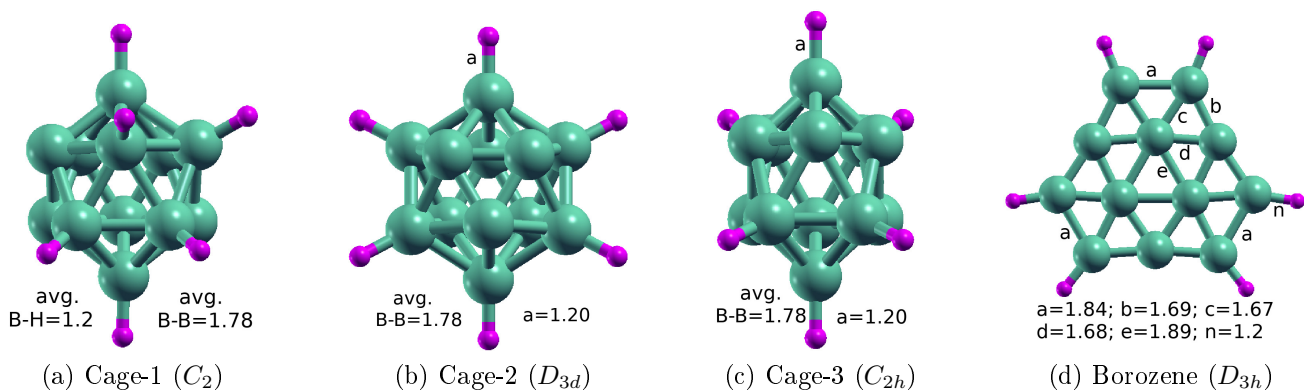


Figure 2: Optimized geometries of various isomers of $B_{12}H_6$ cluster. Structures were optimized at the CCSD level of theory, employing the cc-pVDZ basis sets. The atoms with purple color indicate the hydrogen atoms, and the rest of them are boron atoms. The point group symmetry of the isomers indicated inside parentheses. All the bond lengths are in Å unit.

Table 1: Total energies, and related data for various isomers of $B_{12}H_{12}$ cluster including its di-anion, and $B_{12}H_6$ cluster, are presented below. The point group symmetry of each isomer is shown next to its name. The ground state energies (in Hartree), computed at the CCSD(T) level, and the relative energies (in eV) with respect to their lowest-energy isomers, are also presented. The difference in the total energies of a system at the CCSD(T) and the Hartree-Fock levels of theory, employing cc-pVTZ basis functions, is defined as the correlation energy of that system. The average (avg.) binding energies per atom (in eV) are listed in the last column to indicate the stability of various structures.

Cluster	Isomer	Point group	Ground state energy (Ha)	Relative energy (eV)	Correlation energy (eV)	Avg.Binding energy per atom (eV)
$B_{12}H_{12}$	Neutral Cage	C_i	-304.6848659	0.00	43.44	3.98
	Double ring - 1	D_{6d}	-304.5693208	3.14	43.2	3.85
	Deformed-chain-1	C_2	-304.5368726	4.03	41.17	3.81
	Double ring - 2	D_{6d}	-304.5010969	5.00	46.56	3.77
	Planar triangular	D_{3h}	-304.4501781	6.39	42.48	3.71
	Deformed-chain-2	C_{2h}	-304.3491315	9.14	40.55	3.60
	Cycle	D_{12h}	-303.9550167	19.86	35.04	3.15
$B_{12}H_{12}^{-2}$	Di-anion Icosahedron	I_h	-304.9486026	0.00	42.97	4.28
$B_{12}H_6$	Cage-1	C_2	-300.9978675	0.00	39.42	4.27
	Cage-2	D_{3d}	-300.9903705	0.20	39.44	4.25
	Cage-3	C_{2h}	-300.9490125	1.33	39.08	4.19
	Borozene	D_{3h}	-300.9352434	1.70	37.26	4.17

Results and Discussion

In this section, we present and discuss the results of our calculations for each conformer of $B_{12}H_n$ ($n = 6, 12$) clusters considered in this work, and also the optical properties of the low-lying stable isomers of these clusters. For the $n = 12$ case, in addition to the neutral clusters, we also discuss the case of its di-anion.

$B_{12}H_{12}$ Isomers

Cage

In none of our calculations performed on the cage structures was the optimized geometry found to be a perfect icosahedron, with the I_h point group. However, the geometry optimization performed using the CCSD approach using the cc-pVDZ basis set, predicted a low-symmetry cage with the C_i point group as shown in Fig. 1(a) to have the lowest energy of all the isomers considered. In this structure, the average B-H and B-B bond lengths are 1.2 Å and 1.82 Å, respectively. But, when we performed the vibrational frequency analysis also at the CCSD/cc-pVDZ level of theory, we obtained five imaginary frequencies implying that this structure is completely unstable. We note that long ago Longuet-Higgins and Roberts²¹, based on a simple tight-binding type molecular orbital approach, had also predicted the cage- $B_{12}H_{12}$ with the I_h symmetry to be unstable. Their argument was based on the fact that due to high-symmetry of the structure, the I_h -cage will have degenerate HOMO leading to an open-shell structure, and hence the structural instability. In Fig. 3 we present the energy levels of cage- $B_{12}H_{12}$ with the perfect I_h symmetry, along their electron filling according to the aufbau principle. From the figure it is obvious that due to the four-fold degeneracy, the molecule will have a partially filled HOMO, making it a candidate for Jahn-Teller distortion. However, our geometry optimization calculations go beyond that and have revealed that cage structure of $B_{12}H_{12}$, even with a lower symmetry (C_i), is unstable.

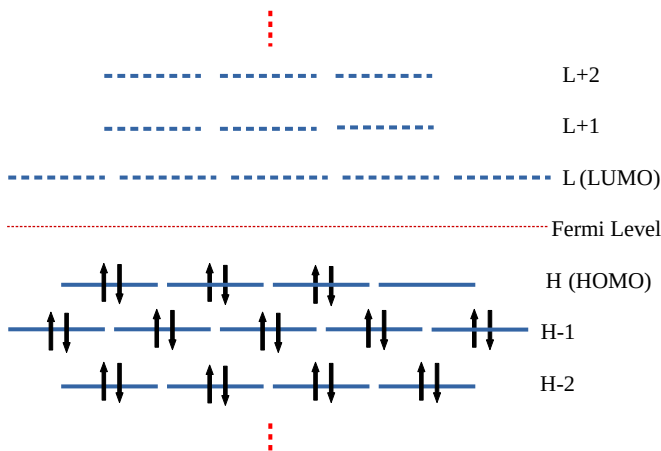


Figure 3: Energy levels of the $B_{12}H_{12}$ cage of perfect icosahedral symmetry (I_h point group), computed using the STO-3G basis, and no electrons. Because the HOMO is four-fold degenerate, there are not enough electrons in the molecule to form a closed-shell structure, leading to its instability.

Deformed chain

The neutral chain-type isomer of $B_{12}H_{12}$ considered in this work is named as “deformed chain”, because of its three-dimensional structure similar to that of a curved (and not straight) chain (see Fig. 1(c)) The geometry of this isomer called deformed-chain-1 shown in Fig. 1(c) was optimized using the DFT, in which we employed the B3LYP exchange-correlation functional, along with the 6-31+G* basis set, and the final structure belongs to the C_2 point group. We also performed the vibrational frequency analysis at the same level of theory, which predicted this structure to be a stable one. The average nearest-neighbor B-B distance is 1.68 Å, while the B-H bond length is 1.22 Å.

However, when we performed the geometry optimization at the CCSD/cc-pVDZ level of theory, we obtained a totally different deformed-chain structure called deformed-chain-2, as depicted in Fig. 1(d), with a planar geometry, and C_{2h} point group. This isomer has average B-B and B-H bond lengths of 1.68 Å, and 1.24 Å, respectively. However, on performing vibrational frequency analysis at the same level of theory, we found that the structure is unstable.

Because deformed-chain-1 (Fig. 1(c)) was found to be stable at the DFT-B3LYP level

of theory, we also computed its optical absorption spectrum using the TDDFT approach, at the same level of theory, and the results are presented in Fig. 4 and Table 2.

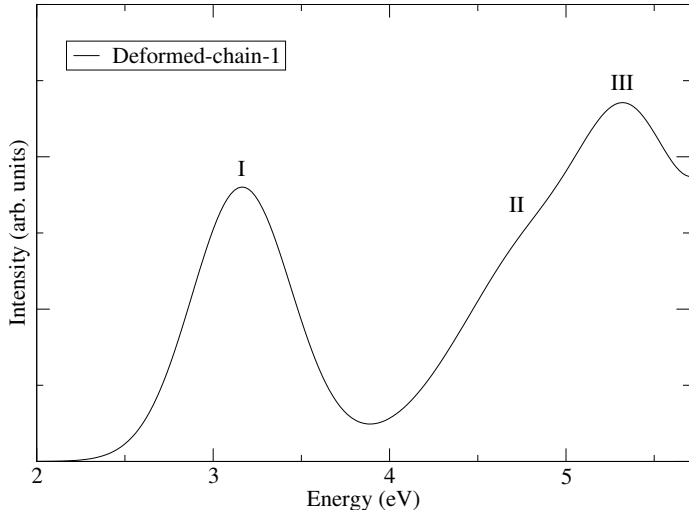


Figure 4: Optical absorption spectrum of the deformed-chain-1 ($B_{12}H_{12}$) isomer, computed using the TDDFT approach, at the B3LYP/6-31+G* level of theory.

Table 2: Excitation energies of the peaks with significant intensities in the optical absorption spectrum of the deformed-chain-1 isomer of $B_{12}H_{12}$ presented in Fig. 4, along with the corresponding oscillator strengths (OS). Additionally, the main configurations contributing to the many-body wave functions of the excited states corresponding to the peaks of the absorption spectrum.

Peak	Energy (eV)	OS	Wave function
I	3.16	0.222	$ H \rightarrow L\rangle$
II	4.81	0.121	$ H \rightarrow L + 2\rangle$
III	5.36	0.097	$ H \rightarrow L + 5\rangle$

From the excited-state wave functions presented in Table 2, it is obvious that the peaks appearing in the absorption spectrum are mainly due to the single excitations from the HOMO of the isomer. The absorption starts with a intense peak at 3.16 eV, dominated by the transition $|H \rightarrow L\rangle$. It is followed by a shoulder peak near 4.80 eV due to the transition

$|H \rightarrow L + 2\rangle$, while the most intense peak near 5.36 eV is characterized by the transition $|H \rightarrow L + 5\rangle$. All the orbitals of this isomer are non-degenerate.

Double ring - 1

This conformer consists of two hexagonal rings of boron (B) atoms kept on top of each other, but in a staggered configuration with the relative twist angle of almost 30° , and each boron atom bonded with one hydrogen atom as shown in Fig. 1(b). This isomer has D_{6d} point group symmetry, with its total energy 3.14 eV higher as compared to the neutral cage conformer. The distances between the two closest in-plane and out-of-plane B-atoms are 1.82 and 1.78 Å, whereas the uniform B-H bond length of the geometry is 1.23 Å. The perpendicular distance between the planes containing two rings is 1.51 Å. The H-B-B-H dihedral angle, where the B- and H-atoms are closest as well as out-of-plane atoms, is 1.08° . Though the B-B bond length of this isomer is larger as compared to our earlier studied stable structure of the bare B_{12} -double ring, the point group symmetry (D_{6d}) remains unchanged.² This geometry was found to be unstable both at the CCSD/ cc-pVDZ as well as B3LYP/6-31+G* levels of theory.

Double ring - 2

This isomer has a very similar structure as double-ring - 1 isomer discussed above, with a larger in-plane B-B atom bond length of 1.87 Å and shorter out-of-plane B-B atom distance of 1.70 Å presented in Fig. 1(e). The uniform B-H bond length of this isomer has also reduced, in comparison, to 1.21 Å. While both the double ring isomers of the $B_{12}H_{12}$ cluster have D_{6d} point group symmetry, but the H-B-B-H dihedral angle of this isomer is comparatively larger (59.46°). This isomer is predicted to be 5.00 eV higher in energy as compared to the neutral cage structure. The perpendicular distance between the planes containing the two rings is 1.40 Å. This structure was also found to be unstable because the vibrational analysis performed at the CCSD as well as DFT (B3LYP) levels of theory led to imaginary

frequencies.

Planar triangular

This conformer is about 6.39 eV higher in energy as compared to the neutral cage isomer, with a D_{3h} point group symmetry. It is composed of an inner-ring of three boron atoms, an outer-ring of nine boron atoms, six in-plain hydrogen atoms, and six out-of-plain hydrogen atoms. From Fig. 1(f), it is evident that the outer-ring consists of two different bond lengths, *i.e.*, 1.70 Å and 1.75 Å, while the inner-ring is composed of one type of bond length (1.98 Å). The connecting bonds between the outer-ring and the inner-ring boron atoms are of two types, *i.e.*, 1.60 Å and 1.86 Å. For the six in-plain hydrogen atoms, the B-H bond length is 1.19 Å, but for the six out-of-plain hydrogen atoms, the B-H bond distance is found to be 1.22 Å. The bare B_{12} - quasi-planar isomer which we studied earlier², also has a similar structure, except that three boron atoms of the inner-ring are out of the plain, whereas all the boron atoms of this structure are in the same plain. However, both CCSD as well as DFT-B3LYP calculations predict this isomer to be unstable.

Cycle

This isomer has a completely planar geometry with the D_{12h} point-group symmetry, and the structure is presented in Fig. 1(g). It is 19.86 eV higher in energy as compared to the neutral cage structure. Clearly, the twelve boron atoms are placed on a circle, with each hydrogen atom attached to a boron atom in the same plain. The uniform bond length between two consecutive boron atoms is found to be 1.79 Å, while the bond distance between the boron and hydrogen atoms is 1.22 Å. But, the vibrational analysis based calculations performed both using the CCSD and the DFT-B3LYP approaches predicted this isomer also to be unstable.

Di-anion Icosahedron ($B_{12}H_{12}^{-2}$)

In Fig. 3 we saw that the neutral $B_{12}H_{12}$ was short of a closed-shell structure by two electrons. Therefore, the question arises whether perfect icosahedral dianion $B_{12}H_{12}^{-2}$ will be stable? Longuet-Higgins and Roberts²¹ had indeed speculated this ion to be stable, because of its closed-shell structure. Later on, Pitochelli and Hawthorne experimentally isolated the dianion $B_{12}H_{12}^{-2}$, and identified it as having the icosahedral structure.²²

To probe this matter, we performed CCSD-based geometry optimization on the cage structure of $B_{12}H_{12}^{-2}$, and obtained the final geometry shown in Fig. 1(h), which has a perfect icosahedral shape with the I_h point group symmetry. As shown in the figure, the optimized B-B bond length is 1.81 Å, whereas the B-H bond length is 1.22 Å. We also performed vibrational frequency analysis on this structure using again CCSD/cc-pVDZ level of theory, and obtained all the frequencies to be real, confirming the stability of this perfect icosahedral structure of $B_{12}H_{12}^{-2}$. Additionally, we also computed the energies of other geometries of $B_{12}H_{12}^{-2}$, and found the energy of the I_h structure to be the lowest. We also computed the first ionization potential of the icosahedral $B_{12}H_{12}^{-2}$ at the CCSD(T)/cc-pVTZ level of theory, and the calculated value of 2.03 eV suggests that the molecule is fairly stable against the ionization as well.

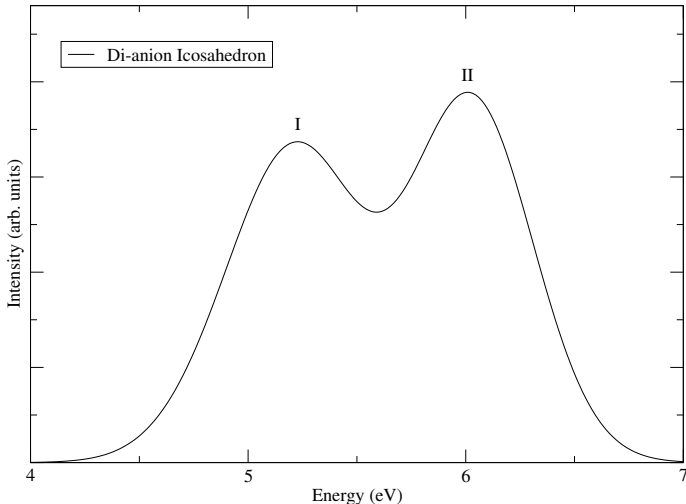


Figure 5: The optical absorption spectrum of di-anion icosahedron isomer calculated using the TDDFT approach at B3LYP/6-31+G* level of theory.

Given the stability of this molecule, we computed its photo-absorption spectrum at the B3LYP/6-31+G* level of theory, the results of which are presented in Fig. 5. The descriptions of the excitations contributing to various peaks are presented in Table 3. From the figure and the table it is obvious that the absorption spectrum of this conformer mainly consist of two intense peaks located near 5 eV and 6 eV. Given the fact that both the peaks are at significantly higher energies than the first ionization potential of the ion (2.03 eV), we conclude that it will be impossible to measure these peaks experimentally.

Table 3: The locations of the peaks with significant intensities in the optical absorption spectrum of the di-anion icosahedral $B_{12}H_{12}^{-2}$ computed using the TDDFT approach, along with the corresponding oscillator strengths (OS), and the wave functions of the excited states.

Peak	Energy (eV)	OS	Wave function
I	4.97	0.034	$ H \rightarrow L + 2\rangle$
	5.26	0.114	$ H - 1 \rightarrow L + 1\rangle$
II	6.03	0.157	$ H - 1 \rightarrow L + 3\rangle$

$B_{12}H_6$ Isomers

In this section we discuss the ground-state geometries of four stable isomers of $B_{12}H_6$, optimized at the CCSD level of theory. We note that out of the four, three conformers have cage-like structures, while the fourth one known as borozene, has a perfectly planar geometry. Furthermore, we found all the four conformers to be vibrationally stable. Therefore, to study their optical properties, we also computed their photoabsorption spectra using the TDDFT approach.

Cage - 1

This lowest energy conformer of the $B_{12}H_6$ cluster belongs to the C_2 point group, and has a cage-type appearance presented in Fig 2(a). Six of the twelve boron atoms are bonded with one hydrogen atom each, with the average B-H bond length 1.20Å. The average B-B bond distance is found to be 1.78 Å. As discussed in our earlier work,² the HOMO orbital

of the isolated icosahedral B_{12} structure has a five-fold degeneracy, of which three orbitals are unoccupied, thus making it unstable against the Jahn-Teller distortion. However, the if we add six more electrons to the system by attaching six hydrogen atoms, the resultant $B_{12}H_6$ cage, will be stable against the distortion because of its closed-shell structure. Indeed, the vibrational frequency analysis performed at the CCSD/cc-pVDZ level of theory predicts that this isomer has a stable structure, without any imaginary frequency.

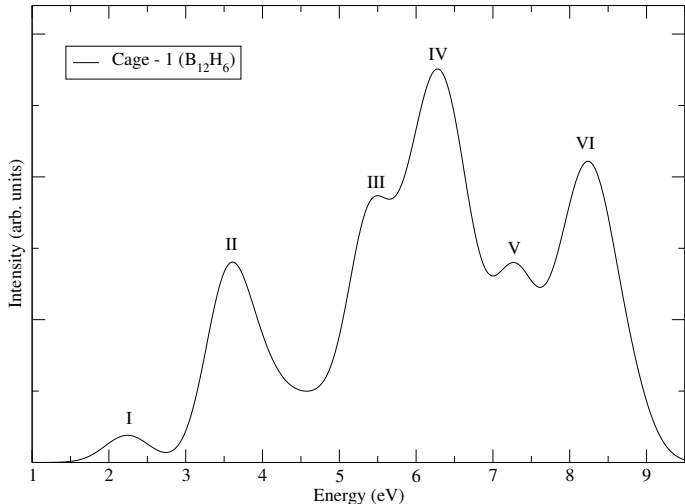


Figure 6: The optical absorption spectrum of cage-1 ($B_{12}H_6$) isomer calculated using the TDDFT approach at B3LYP/6-31+G* level of theory.

Table 4: Peak locations in the optical absorption spectrum of cage-1 isomer of the $B_{12}H_6$ cluster, computed using the TDDFT approach, along with the corresponding oscillator strength (OS), and the wave functions of the excited states contributing to the peaks.

Peak	Energy (eV)	OS	Wave function
I	2.18	0.013	$ H \rightarrow L + 2\rangle$
	2.31	0.011	$ H \rightarrow L + 1\rangle$
II	3.52	0.135	$ H \rightarrow L + 3\rangle$
III	5.35	0.120	$ H \rightarrow L + 4\rangle$
IV	6.16	0.067	$ H - 9 \rightarrow L + 1\rangle$
	6.52	0.065	$ H \rightarrow L + 16\rangle$
V	7.28	0.064	$ H \rightarrow L + 19\rangle$
VI	8.29	0.053	$ H - 1 \rightarrow L + 12\rangle$

The calculated optical absorption spectrum of this isomer is shown in Fig. 6, whereas information related to various peaks is represented in Table 4. It is obvious from the table

that several peaks occur due to transition from the HOMO to the virtual orbitals. The absorption spectrum starts with a small peak near 2.20 eV due to two close-lying excited states whose wave functions consist mainly of the single excitation $|H \rightarrow L + 2\rangle$ and $|H \rightarrow L + 1\rangle$. It is followed by two moderately intense peaks at 3.52 and 5.35 eV that are dominated by the transitions $|H \rightarrow L + 3\rangle$ and $|H \rightarrow L + 4\rangle$, respectively. The most intense peak near 6.50 eV is due to two excited states characterized by the transitions $|H - 9 \rightarrow L + 1\rangle$ and $|H \rightarrow L + 16\rangle$. The peaks at 7.28 and 8.29 eV are largely composed of the singly excitations $|H \rightarrow L + 19\rangle$ and $|H - 1 \rightarrow L + 12\rangle$, respectively. All the molecular orbitals involved in optical transitions of this isomer are non-degenerate.

Cage - 2

This isomer of the $B_{12}H_6$ cluster presented in Fig. 2(b), which also has a cage geometry with a D_{3d} point group symmetry, is only 0.2 eV higher than its lowest-energy conformer. The average optimized lengths of the B-B and B-H bonds are 1.78 Å, and 1.20 Å, respectively. According to the CCSD/cc-pVDZ level vibrational frequency analysis, this isomer is completely stable. Therefore, we calculated its optical absorption spectrum shown in Fig. 7, while the dominant configurations contributing to its peaks are presented in Table 5.

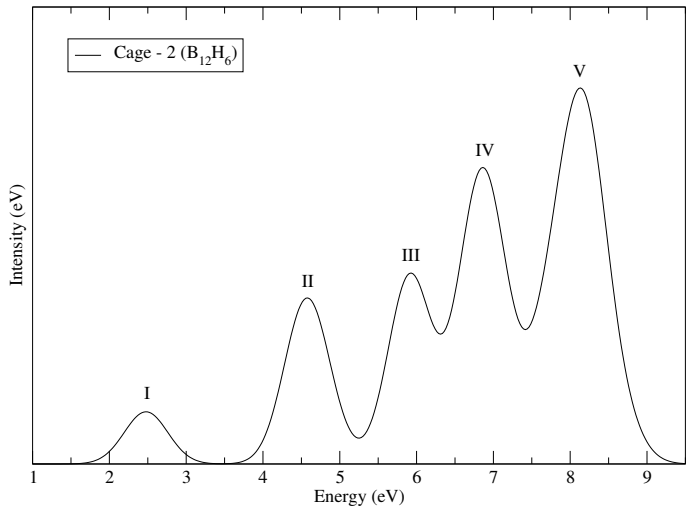


Figure 7: The optical absorption spectrum of cage-2 $B_{12}H_6$ isomer calculated using the TDDFT approach at B3LYP/6-31+G* level of theory.

Table 5: Peak locations of the optical absorption spectrum of cage-2 isomer of the $B_{12}H_6$ computed using the TDDFT approach, along with the corresponding oscillator strength (OS), and the wave functions of the excited states contributing to its peaks.

Peak	Energy (eV)	OS	Wave function
I	2.48	0.028	$ H - 1 \rightarrow L\rangle$
II	4.53	0.070	$ H \rightarrow L + 1\rangle$
III	5.92	0.201	$ H \rightarrow L + 3\rangle$
IV	6.75	0.130	$ H - 1 \rightarrow L + 6\rangle$
V	7.80	0.096	$ H - 9 \rightarrow L\rangle$
	8.19	0.120	$ H - 1 \rightarrow L + 12\rangle$

The absorption begins with a small peak at 2.48 eV due to the transition $|H - 1 \rightarrow L\rangle$, where $|H - 1\rangle$ is non-degenerate but $|L\rangle$ is doubly degenerate. Peak II appears due to the state whose wave function is largely composed of the $|H \rightarrow L + 1\rangle$ transition. The $|L + 1\rangle$ is also doubly degenerate. It is followed by two moderately intense peaks at 5.92 and 6.75 eV characterized by the transitions $|H \rightarrow L + 3\rangle$ and $|H - 1 \rightarrow L + 6\rangle$, respectively. The most intense peak of the spectrum near 8 eV is due to two excited states, dominated by the single excitations $|H - 9 \rightarrow L\rangle$ and $|H - 1 \rightarrow L + 12\rangle$, where both $|H - 9\rangle$ and $|L + 12\rangle$ are doubly degenerate. This most intense peak is also associated with the orbitals, which are far away from the Fermi level.

Cage - 3

This isomer is 1.33 eV higher in energy as compared to the lowest-energy cage-1 isomer, with the C_{2h} point group symmetry. The optimized geometry is presented in Fig. 2(c), and in that the average bond length between two boron atoms is 1.78 Å, while that between boron and hydrogen atoms is 1.20 Å. The vibrational frequency analysis predicts that this structure is also a stable one, and its optical absorption spectrum is presented in Fig. 8, while the information related to the peaks is represented in Table 6.

The absorption starts with a small peak at 1.77 eV, dominated by the transition $|H - 1 \rightarrow L\rangle$. It is followed by an intense peak near 4.10 eV due to the transitions $|H \rightarrow L + 2\rangle$ and $|H \rightarrow L + 3\rangle$. The peak-III at 5.61 eV is due to the state whose wave function consists

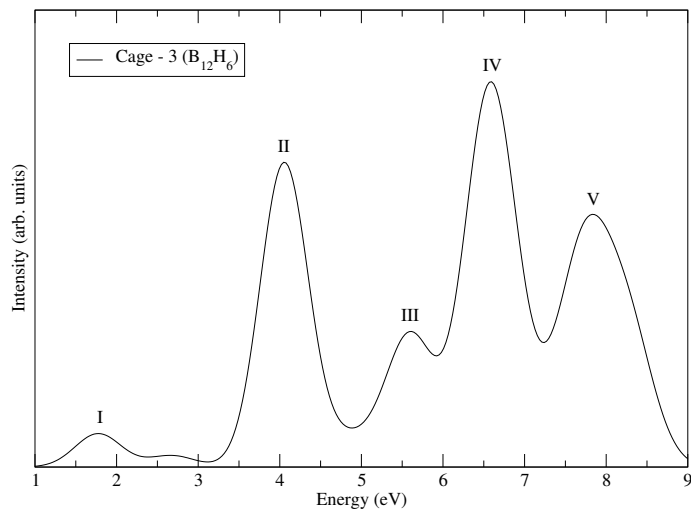


Figure 8: The optical absorption spectrum of cage-3 ($B_{12}H_6$) isomer calculated using the TDDFT approach at B3LYP/6-31+G* level of theory.

Table 6: The peak locations of the optical absorption spectrum of cage-3 isomer of the $B_{12}H_6$ computed using the TDDFT approach, along with the corresponding oscillator strength (OS), and the wave functions of the excited states contributing to its peaks.

Peak	Energy (eV)	OS	Wave function
I	1.77	0.027	$ H - 1 \rightarrow L\rangle$
II	4.00	0.172	$ H \rightarrow L + 2\rangle$
	4.17	0.081	$ H \rightarrow L + 3\rangle$
III	5.61	0.090	$ H \rightarrow L + 5\rangle$
IV	6.42	0.081	$ H - 11 \rightarrow L\rangle$
	6.57	0.064	$ H \rightarrow L + 14\rangle$
	6.62	0.056	$ H - 1 \rightarrow L + 9\rangle$
V	7.67	0.062	$ H - 1 \rightarrow L + 17\rangle$
	7.79	0.052	$ H - 1 \rightarrow L + 18\rangle$

mainly of the configuration $|H \rightarrow L + 5\rangle$. The most intense peak, *i.e.*, peak IV is due to the three excited states dominated by the transitions $|H - 11 \rightarrow L\rangle$, $|H \rightarrow L + 14\rangle$, and $|H - 1 \rightarrow L + 9\rangle$. The final peak (V) of the spectrum is due to two excited states, whose wave functions are largely composed of the transitions $|H - 1 \rightarrow L + 17\rangle$ and $|H - 1 \rightarrow L + 18\rangle$. Obviously, peaks IV and V involve orbitals which are far away from the Fermi level. All the orbitals of this conformer are non-degenerate.

Borozone

By means of first-principles calculations, Szwacki *et al.*⁷ were the first to propose the existence of a completely planar isomer of $B_{12}H_6$, with D_{3h} point group symmetry, which, in analogy with benzene, they called borozone. We performed geometry optimization of this isomer at the CCSD/cc-pVDZ level of theory, and, in agreement with Szwacki *et al.*⁷, found the structure to have D_{3h} symmetry (see Fig 2(d)), with the total energy 1.7 eV higher than that of the cage-1 structure. The outer-ring is composed of two types of B-B bond lengths, *i.e.*, 1.84 Å and 1.69 Å, while the inner ring has uniform B-B bond lengths 1.89 Å. The connecting bonds between the inner ring and the outer ring boron atoms are also of two kinds, *i.e.*, 1.67 Å and 1.68 Å, which differ very slightly from each other. The uniform B-H bond length in the structure is 1.20 Å. We also carried out the vibrational frequency analysis using the CCSD approach, and the cc-pVDZ basis set, and found it to be a stable structure. This isomer has a geometry very similar to that of the triangular $B_{12}H_{12}$ discussed above, except for the six non-planar hydrogen atoms, and slightly different B-B and B-H bond lengths.

In an earlier work from our group, Sahu *et al.*⁸ reported the structure of borozone, optimized at the INDO-HF level of theory, to have uniform B-B and B-H bond lengths of 1.65 Å and 1.18 Å, respectively. They also optimized the structure at the B3LYP/6-311++g(d) level of theory, and found it to have four distinct B-B bond lengths 1.63 Å, 1.66 Å, 1.81 Å, and 1.86 Å, in addition to the uniform B-H bond length 1.18 Å.⁸ Clearly, these values are in very good agreement with our CCSD-level optimized geometry parameters.

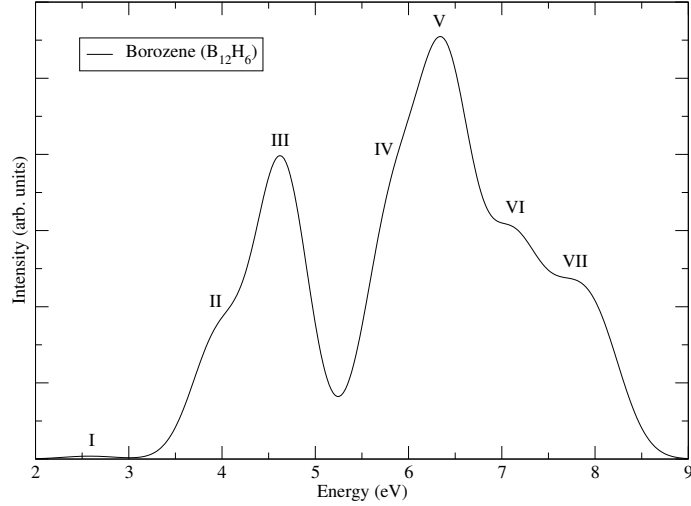


Figure 9: The optical absorption spectrum of borozene ($B_{12}H_6$) isomer calculated using the TDDFT approach at B3LYP/6-31+G* level of theory.

Table 7: The peak locations of the optical absorption spectrum of borozene isomer of the $B_{12}H_6$ computed using the TDDFT approach, along with the corresponding oscillator strength (OS), and the wave functions of the excited states contributing to its peaks.

Peak	Energy (eV)	OS	Wave function
I	2.58	0.005	$ H \rightarrow L\rangle$
II	3.96	0.096	$ H - 1 \rightarrow L\rangle$
III	4.64	0.240	$ H - 1 \rightarrow L + 1\rangle$
IV	5.79	0.166	$ H \rightarrow L + 3\rangle$
V	6.34	0.195	$ H \rightarrow L + 4\rangle$
VI	7.14	0.104	$ H \rightarrow L + 9\rangle$
VII	8.00	0.066	$ H \rightarrow L + 14\rangle$

Our calculated absorption spectrum of this isomer (Fig. 9) starts at 2.58 eV, with a weak peak (I), followed by two major peaks labeled III, and V, along with several shoulders with comparable intensities which broaden the spectrum. The location of peak I at 2.58 eV is in excellent agreement with the value 2.6 eV reported by Szwacki *et al.*⁷. Because of the strictly planar structure of borozene, its orbitals can be classified as either of π type, or of σ type. On inspection we find that HOMO-1, HOMO, LUMO, LUMO+1, LUMO+2, and LUMO+3 are all of π type, while the immediately lower/higher orbitals are of σ type. As far as orbitals further away from the Fermi level are concerned, they were found to be of either type. The information related to various features of the calculated spectrum of borozene is presented in Table 7, from where it is obvious that the first peak dominated by the HOMO (H) to LUMO (L) transition is a π - π^* excitation. Peak II at 3.96 eV is due to a state whose wave function consists mainly of the configuration $|H-1 \rightarrow L\rangle$, while the moderately intense peak near 4.6 eV is primarily composed of the configuration $|H-1 \rightarrow L+1\rangle$. Clearly, both these peaks correspond again to π - π^* transitions. They are followed by a peak (IV) near 5.80 eV characterized by the excitation $|H \rightarrow L+3\rangle$, which is also a π - π^* transition. The most intense peak at 6.34 eV is identified as a π - σ^* transition, due to an excited state whose wave function is dominated by the single excitation $|H \rightarrow L+4\rangle$. The last two shoulder peaks of the computed absorption spectrum are located at 7.14 and 8.00 eV, whose wave functions are composed mainly of excitations $|H \rightarrow L+9\rangle$ and $|H \rightarrow L+14\rangle$, which are π - π^* and π - σ^* transitions, respectively. In our earlier work⁸, we also computed the optical absorption spectrum of borozene using the INDO model, and the multi-reference-singles-doubles configuration-interaction (MRSDCI) approach. On comparing our INDO/MRSDCI spectrum⁸ to the present one, we note that there are very significant differences between the two. The first peak of the INDO/MRSDCI spectrum was found at 2.25 eV, as compared to 2.58 eV in the present calculation. Furthermore, the rest of the peaks in the INDO/MRSDCI spectrum⁸ were located at energies larger than 7 eV, clearly, in disagreement with the present calculations. Given the larger basis set involved in our present calculations, we are inclined

to trust these first-principles calculations more than our previous INDO-model based work.⁸ However, the disagreement between the two sets of calculations can definitively be resolved only by experimentally measuring the absorption spectrum of borozene.

Based on our calculated spectra, we note that the optical signatures of various isomers of the $B_{12}H_6$ cluster are sufficiently different from each other so that they can be identified using optical spectroscopy.

Conclusions

With the aim of understanding the stability against distortions, we performed electron-correlated calculations on various conformers of $B_{12}H_{12}$ and $B_{12}H_6$ clusters. The geometries of all the isomers were optimized using the CCSD approach and cc-pVDZ basis set. In order to investigate the structural stability, the vibrational frequency analysis was also carried out for all the isomers. According to our calculations, all the four conformers of $B_{12}H_6$ considered in this work are stable, while only the deformed-chain isomer of $B_{12}H_{12}$ is stable. In particular, the perfect icosahedral cage of $B_{12}H_{12}$ (I_h symmetry) cluster was found to be unstable, consistent with the Jahn-Teller analysis. The same analysis suggests that the di-anion $B_{12}H_{12}$, with the perfect I_h symmetry should be stable, in full agreement with our calculations. We also computed the optical absorption spectra of all the stable isomers using the TDDFT approach, and found that they differ significantly from each other, suggesting the possibility of their identification using optical spectroscopy.

Author Information

Corresponding Authors

Alok Shukla: *E-mail: shukla@phy.iitb.ac.in

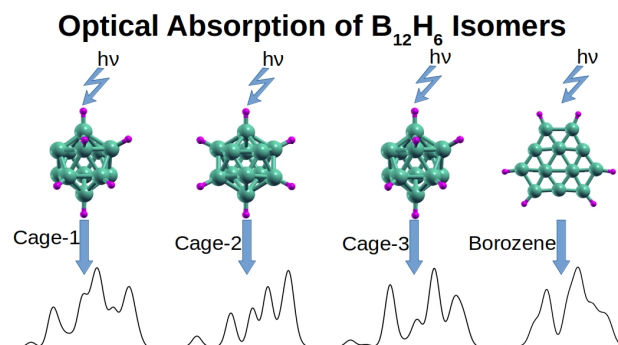
Notes

The authors declare no competing financial interests.

Acknowledgements

Work of P.B. was supported by a Senior Research Fellowship offered by University Grants Commission, India.

TOC Graphic



References

- (1) Liu, S.-Y.; Stephan, D. W. Contemporary Research in Boron Chemistry. *Chem. Soc. Rev.* **2019**, *48*, 3434–3435.
- (2) Bhattacharyya, P.; Boustani, I.; Shukla, A. First principles study of structural and optical properties of B₁₂ isomers. *Journal of Physics and Chemistry of Solids* **2019**, *133*, 108 – 116.
- (3) Lipscomb, W. N.; Massa, L. Examples of large closo boron hydride analogs of carbon fullerenes. *Inorganic Chemistry* **1992**, *31*, 2297–2299.

- (4) Ohishi, Y.; Kimura, K.; Yamaguchi, M.; Uchida, N.; Kanayama, T. Synthesis and formation mechanism of hydrogenated boron clusters B₁₂H_n with controlled hydrogen content. *The Journal of Chemical Physics* **2010**, *133*, 074305.
- (5) Ohishi, Y.; Kimura, K.; Yamaguchi, M.; Uchida, N.; Kanayama, T. Formation of hydrogenated boron clusters in an external quadrupole static attraction ion trap. *The Journal of Chemical Physics* **2008**, *128*, 124304.
- (6) Ohishi, Y.; Kimura, K.; Yamaguchi, M.; Uchida, N.; Kanayama, T. Energy barrier of structure transition from icosahedral B₁₂H₆ to planar B₁₂H₅ and B₁₂H₄ clusters. *Journal of Physics: Conference Series* **2009**, *176*, 012030.
- (7) Szwacki, N. G.; Weber, V.; Tymczak, C. J. Aromatic Borozene. *Nanoscale Research Letters* **2009**, *4*, 1085.
- (8) Sahu, S.; Shukla, A. Probing Aromaticity of Borozene Through Optical and Dielectric Response: A Theoretical Study. *Nanoscale Research Letters* **2010**, *5*, 714.
- (9) Forte, G.; La Magna, A.; Deretzis, I.; Pucci, R. Ab Initio Prediction of Boron Compounds Arising from Borozene: Structural and Electronic Properties. *Nanoscale Research Letters* **2009**, *5*, 158.
- (10) Frisch, M. J. et al. Gaussian 16 Revision C.01. 2016; Gaussian Inc. Wallingford CT.
- (11) Becke, A. D. Density-functional thermochemistry. III. The role of exact exchange. *The Journal of Chemical Physics* **1993**, *98*, 5648–5652.
- (12) Lee, C.; Yang, W.; Parr, R. G. Development of the Colle-Salvetti correlation-energy formula into a functional of the electron density. *Phys. Rev. B* **1988**, *37*, 785–789.
- (13) Stephens, P. J.; Devlin, F. J.; Chabalowski, C. F.; Frisch, M. J. Ab Initio Calculation of Vibrational Absorption and Circular Dichroism Spectra Using Density Functional Force Fields. *The Journal of Physical Chemistry* **1994**, *98*, 11623–11627.

- (14) Bauernschmitt, R.; Ahlrichs, R. Treatment of electronic excitations within the adiabatic approximation of time dependent density functional theory. *Chemical Physics Letters* **1996**, *256*, 454 – 464.
- (15) Hirata, S.; Head-Gordon, M. Time-dependent density functional theory for radicals: An improved description of excited states with substantial double excitation character. *Chemical Physics Letters* **1999**, *302*, 375 – 382.
- (16) Hirata, S.; Head-Gordon, M. Time-dependent density functional theory within the Tamm-Dancoff approximation. *Chemical Physics Letters* **1999**, *314*, 291 – 299.
- (17) Bhattacharyya, P.; Rai, D. K.; Shukla, A. Pariser-Parr-Pople Model Based Configuration-Interaction Study of Linear Optical Absorption in Lower-Symmetry Polycyclic Aromatic Hydrocarbon Molecules. *The Journal of Physical Chemistry C* **2020**, *124*, 14297–14305.
- (18) Mallocci, G.; Cappellini, G.; Mulas, G.; Mattoni, A. Electronic and optical properties of families of polycyclic aromatic hydrocarbons: A systematic (time-dependent) density functional theory study. *Chemical Physics* **2011**, *384*, 19 – 27.
- (19) Mallocci, G.; Mulas, G.; Cappellini, G.; Joblin, C. Time-dependent density functional study of the electronic spectra of oligoacenes in the charge states -1, 0, +1, and +2. *Chemical Physics* **2007**, *340*, 43 – 58.
- (20) Mocci, P.; Cardia, R.; Cappellini, G. A computational study on the electronic and optical properties of boron-nitride circumacenes. *Phys. Chem. Chem. Phys.* **2019**, *21*, 16302–16309.
- (21) Longuet-Higgins, H. C.; Roberts, M. D. V. The electronic structure of an icosahedron of boron atoms. *Proceedings of the Royal Society of London. Series A. Mathematical and Physical Sciences* **1955**, *230*, 110–119.

- (22) Pitochelli, A. R.; Hawthorne, F. M. The isolation of the icosahedral B₁₂H₁₂²⁻ ion.
Journal of the American Chemical Society **1960**, *82*, 3228–3229.